

Optimized ultra-high-performance concrete horizontally curved bridge superstructure

Musa Alawneh, Maher K. Tadros, and Chuanbing (Shawn) Sun

- This paper demonstrates the viability and effectiveness of employing ultra-high-performance concrete production in curved bridges. The focus is on the application of ultra-high-performance concrete for a curved bridge design, as well as proposed simplified production and construction methods.
- A preliminary concept design is presented to demonstrate the use of ultra-high-performance concrete to reduce weight, improve constructibility, and increase durability of curved bridge structures.

Curved bridge alignments are common in complex interchanges. According to a 1991 Structural Stability Research Council survey,¹ 25% of bridges in the United States are curved bridges. They have gained popularity since the early 1960s because they can fit within the limited space of congested urban areas and are aesthetically appealing. Moreover, a curved bridge allows for longer spans, which eliminates part of the substructure. There are several options for superstructure selection of curved bridges: steel I-girders, steel tub girders, cast-in-place concrete box girders, and precast concrete segmental box girders.

Steel bridge girders have dominated the curved bridge field. Their advantages include speed of construction, their relative flexibility, and being lightweight. U.S. contractors and designers are familiar with curved steel bridges owing to extensive research and design aids provided by the steel industry, the Federal Highway Administration (FHWA), and a number of state highway agencies. Curved steel bridges can command a high premium cost because there is a lack of competing precast concrete girder solutions that are as convenient to design and build. The high maintenance costs associated with steel structures are well known.

In the United States, cast-in-place, post-tensioned concrete box-girder bridges are common only in the Southwest. They require extensive fieldwork and specialized formwork and construction crews. In addition, especially in cold weather regions, owners often require a way to remove and replace bridge decks that are deteriorated due to cold weather ef-

fects. Meeting this requirement is difficult with cast-in-place concrete box girders.

Precast concrete segmental bridges are an attractive and cost-effective option only when the bridge length is long enough to justify the investment in segmental box forming, geometric controls, specialized design, construction engineering, and erection equipment. Therefore, the commonly used precast concrete stringer type option seems to be the most attractive solution because this type allows for curved horizontal alignment and for being prestressed at that alignment.²⁻⁵ Investigating this option is one of the two primary goals of this paper. The second is to consider the use of ultra-high-performance concrete (UHPC) to reduce weight, improve constructibility, and increase durability of curved bridge structures.

The precast concrete tub girder is an attractive alternative to the steel plate I-girders or tub girders. This precast concrete product has been tried successfully in Nebraska⁶ (**Fig. 1**), Colorado,^{7,8} and Florida (**Fig. 2**), and it has been introduced as a PCI Zone 6 standard.⁹ It has also been shown to be competitive with conventional curved steel bridges.¹⁰

Despite the success of the recent U beam bridges shown in Fig. 1 and 2, the authors believe that future designs can be further simplified to reduce cost and construction time. In

this paper, we aim to show that spans up to 240 ft (73 m) can be erected without intermediate shoring. Also, elimination of draped post-tensioning in the webs can significantly decrease the web widths and reduce the risk of defects in the post-tensioning grouting, which can cause strand corrosion. This paper also addresses the challenge that the “perfect” solution of providing continuously curved sides of the beam is difficult and expensive. Horizontal curvature cannot always be kept constant, even in the same bridge between various girder lines. Thus, the authors propose to use a series of straight segments that are kinked at the joints. This concept was successfully used on the Arbor Road Bridge in Nebraska,⁶ in which 40 ft (12 m) straight segments were used on a 1200 ft (366 m) curvature radius. It is difficult for the driving public to discern between a chorded girder bridge and a truly curved bridge (**Fig. 1**). If the segments are made straight in a standard bed, the precast concrete plant’s need for capital improvements is minimized. When designers are given adequate guidance and design tools, they will be encouraged to specify precast concrete girders as a cost-effective alternative. Finally, if limitations to certain precast concrete section shapes are provided to designers, the precast concrete girder system can be expanded to long spans and sharply curved bridges.¹¹

In bridges with significant curvature, the girders can be subjected to large torsional moments. Certain beams, such as U and I-beams, are not efficient for resisting torsion due



Figure 1. Arbor Road over Interstate 80 bridge near Lincoln, Neb. The curved alignment was made with straight, chorded 40 ft long segments. Source: Reproduced from Sun et al. (2007). Note: 1 ft = 0.305 m.

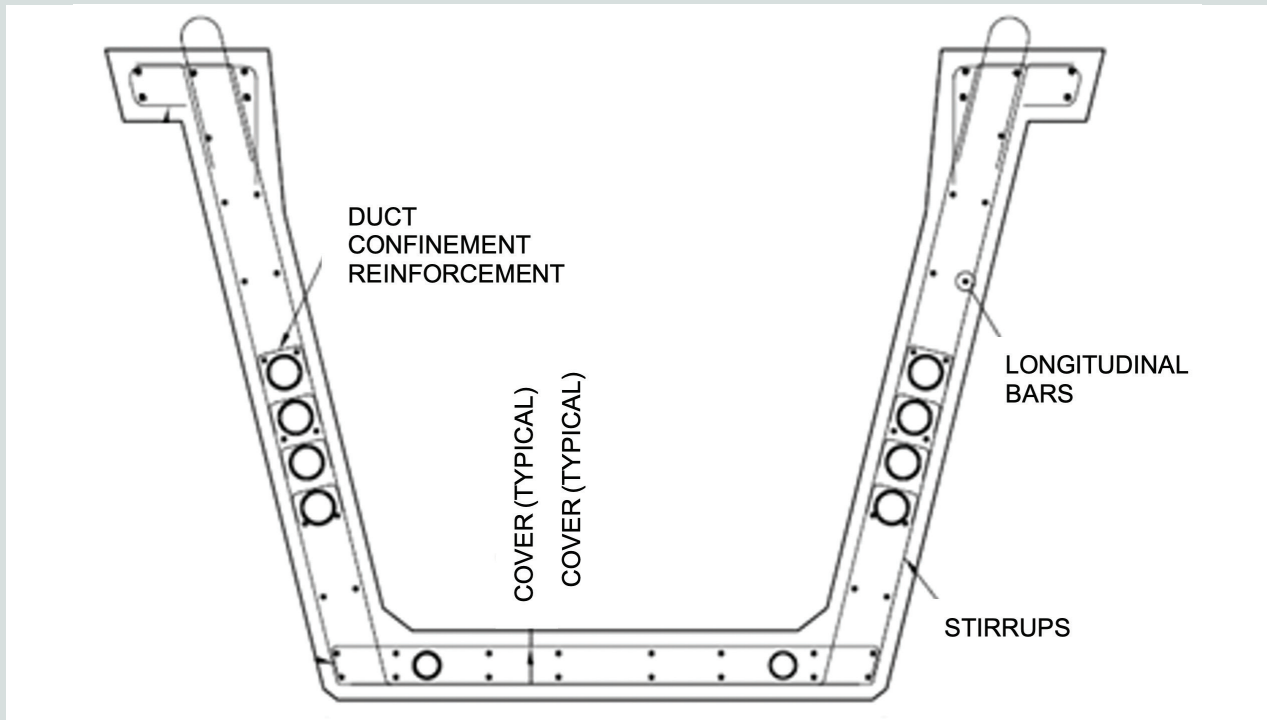


Figure 2. Typical reinforcement of bridge cross section in Florida. Note: 1" = 1 in. = 25.4 mm.

to their open cross-section shape and relatively low torsional rigidity. Box beams are the most efficient section shapes, but they are harder to precast than U beams. Thus, the deck slab is an important component of the torsional resistance in a U beam system because it converts the U shape to a box shape. This condition, however, is only available after the deck hardens and becomes part of the structure. Thus, the beam is relatively weak for the effects of its own weight and the weight of the fresh deck concrete, which are nearly two-thirds of the total load. In the paper by Alawneh et al.¹¹ and the discussion later in this paper, it is recommended that a box section be made in the precast concrete plant before it is shipped to the site.

UHPC is a new class of concrete that relies on a highly refined microstructure and fiber reinforcement to achieve superior performance characteristics, including high compressive strength and superior postcracking tensile strength and ductility.¹² The extremely low permeability of the concrete provides exceptional long-term durability in aggressive environments. Despite these advantageous characteristics, applications of UHPC in the United States have been primarily limited to joints between precast concrete bridge deck panels and a small number of demonstration projects in a few states, such as Iowa and Virginia. The high material cost and a shortage of national design guidelines have been obstacles to widespread acceptance of this material. In the United States, the first UHPC bridge was built in 2006 in Wapello County, Iowa, as a collaboration between the FHWA and the Iowa Department of Transportation. In 2008, an I-girder made of UHPC was used in a bridge over Cat Point Creek in Richmond County, Va.

In 2018, PCI awarded a major research project to develop materials and structural design guidelines for implementation of UHPC in long-span pretensioned concrete bridge and building members. The project team includes researchers from two architecture and engineering firms, the University of Nebraska, Ohio State University, North Carolina State University, and Louisiana Tech University, as well as five precast concrete companies in the United States and one precast concrete company in Canada. Research was completed in May 2021, and the final report was approved by the PCI Research and Development Council in September 2021. Findings¹⁴ from the research are encouraging. It is possible to have a UHPC mixture designed with locally sourced raw materials and made for about one-third the cost of previously available proprietary prebagged materials. For example, it is possible to make a UHPC mixture for about \$800 per cubic yard (\$1046 per cubic meter). This could allow the product costs for UHPC to rival those of conventional concrete. If concrete volume is optimized in UHPC to correspond to 50% of conventional concrete members and the UHPC product is sold at \$1500 per cubic yard (\$1962 per cubic meter), compared with \$750 per cubic yard (\$981 per cubic meter) for a conventional concrete product, the product costs would be the same. This example becomes even more attractive when considering all the additional benefits of UHPC, including significant cost savings for production labor, shipping, foundations, shoring, and so on. Most significantly, life-cycle costs are greatly reduced with UHPC, as demonstrated by Voo and Foster.¹⁵ They show that UHPC structural members produce lower carbon dioxide emissions, less embodied energy, and less climate change

potential than structural steel and conventional concrete members. In addition, UHPC members allow for enhanced structural durability and increased service life.¹⁴ Very few reinforcing bars are required, significantly reducing labor in engineering and production.

A significant disadvantage of curved precast concrete girders is their heavy weight, which necessitates that pieces be made shorter than span length and intermediate shoring be used, risking interference with live vehicular and truck traffic. Using the proposed relatively large number of beams per span results in a relatively small cross section and lighter member weight. When UHPC is used, member weight is further reduced. This paper will theoretically show that a 240 ft (73 m) long full span can be erected in one piece weighing less than 150 tons (136,200 kg) without any need for intermediate shoring.

Material properties of the UHPC used in the bridge example

The concrete assumed to be used in this example is consistent with the specifications developed for the PCI UHPC report¹⁴ and successfully batched by six major precasters in the United States and Canada. The minimum properties are as follows:

- Compressive strength at service is 17.4 ksi (120 MPa).
- Tensile properties are based on ASTM C1609, *Standard Test Method for Flexural Performance of Fiber-Reinforced Concrete (Using Beam with Third-Point Loading)*¹⁶ (Fig. 3). The load deflection graph must demonstrate strain hardening. The extreme fiber stress limit equals 1.5 ksi (10.3 MPa) at first cracking and 2.0 ksi (13.8 MPa) at peak load, with both limits calculated based on linear elastic analysis as per ASTM C1609.

- Modulus of elasticity is 5000 ksi (34,475 MPa) at initial loading and 6500 ksi (44,818 MPa) at service, unless shown otherwise by testing.
- Following ASTM A615, *Standard Specification for Deformed and Plain Carbon-Steel Bars for Concrete Reinforcement*,¹⁷ the seven-wire strands are 0.6 in. (15 mm) in diameter with an area of 0.217 in.² (140 mm²) and a modulus of elasticity E_{ps} of 28,500 ksi (196,508 MPa).
- Reinforcing bars are as specified in ASTM A1035, *Standard Specification for Deformed and Plain, Low-Carbon, Chromium, Steel Bars for Concrete Reinforcement*,¹⁸ (also known as ChromX 9100 bars), with 100 ksi (690 MPa) yield strength and a modulus of elasticity E_s of 29,000 ksi (199,955 MPa). This grade is not a requirement of PCI UHPC. It is preferred and is used in the example in this paper.

Design of UHPC curved bridges

Curved bridge beams are subjected to combined shear and torsion. Thin-webbed I-beams and open-top U beams have been popular for straight beams, but they have relatively low torsional stiffness and, unless provided with high levels of

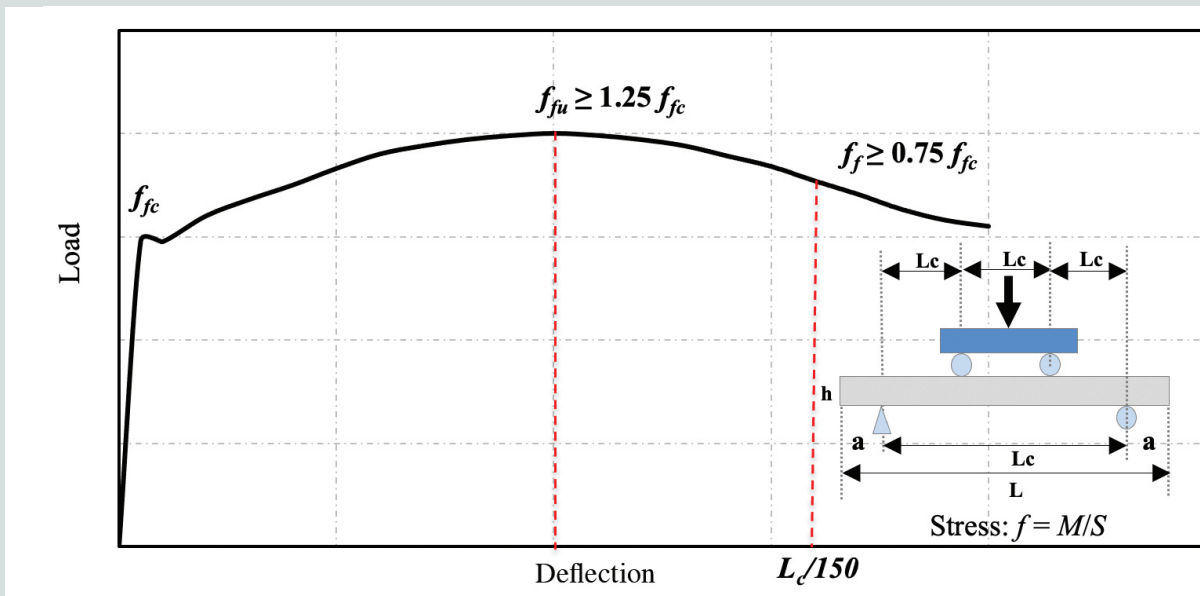


Figure 3. Load-deflection graph according to ASTM C1609, with minimum PCI ultra-high-performance concrete properties identified. Note: a = distance from centerline of support to end of beam; f = beam stresses at extreme fibers; f_c = tensile stress corresponding to certain load during the flexural strength test; f_{fc} = first-peak (first crack) flexural strength; f_{fu} = peak flexural tensile strength; h = depth of specimen; L = total length of specimen; L_c = distance between supports of specimen; M = bending moment; S = section modulus.

prestress, are likely to crack in torsion due to deck weight while only the precast concrete member is available to resist loads. For sharply curved beams, as in the example discussed in this paper, it is advisable to have a precast concrete box beam. The precasting operation can still be done in two stages, or expanded polystyrene foam block can be used to form the void. Collapsible internal steel forms have also been used by precasters to form the void. Collapsible steel forms are particularly attractive for the system being described in this paper because all segments are relatively short and straight.

As mentioned, conventional concrete curved U beams have been successfully constructed in Colorado and Florida (Fig. 2). These beams have relatively wide (8 to 10 in. [203 to 254 mm]) webs to accommodate post-tensioning ducts plus four layers of reinforcing bars. In the proposed system, no post-tensioning ducts in the webs are used and very few reinforcing bars are used only in the ends at the post-tensioning anchors. The use of UHPC allows for the virtual elimination of stirrups, as shown in the calculations later in this paper. After several iterations, the final web width was found to be 4 in. (102 mm). This is a major development and has far-reaching impacts. It allows for assembly on the ground of long beam segments, perhaps the entire span, without need for temporary shoring. This is advantageous because temporary shoring slows construction and could interfere with traffic. Also, if the shoring settles, it can have a negative impact on the entire bridge.

The analysis of curved bridges constructed with UHPC is similar to the analysis of conventional precast concrete bridges. The cross-section dimensions and member weight are smaller when UHPC is used, and that provides benefits related to structural demand, transportation, handling, temporary supports, and foundations. UHPC design is also similar to conventional post-tensioned concrete design, except for shear and torsion. When designing for these effects, it is possible to eliminate the stirrups used with conventional concrete due to the high shearing (diagonal tension) contributions of the fibers, as long as the previously stated tensile properties are met. Readers may refer to Alawneh¹⁹ for a more detailed discussion of behavior and analysis methods of curved precast concrete stringer bridges. The theory presented there will not be reviewed in this paper. Rather, the focus is on its application to UHPC, as well as simplified production and construction methods.

Flexural tension of UHPC is greatly enhanced by the presence of high-strength steel fibers (Fig. 3). In this design, the tensile stress limits are set in accordance with the design guidelines of the PCI UHPC report.¹⁴ They are 0.75 ksi (5.2 MPa) at the time of post-tensioning and 1.00 ksi (6.9 MPa) at service, as indicated in the design criteria section later in this paper. These are conservative values, less than the 1.5 ksi (10.3 MPa) minimum required cracking stress determined by ASTM C1609.¹⁶ The PCI UHPC report¹⁴ also specifies that ductility strain hardening be ensured (Fig. 3) consistently with recommendations by Gowripalan and Gilbert²⁰ and with

provisions for fiber-reinforced concrete allowed to resist shear without minimum stirrups in the American Concrete Institute's *Building Code Requirements for Structural Concrete (ACI 318-19) and Commentary (ACI 318R-19)*.²¹

Strength limit state

By referring to a typical stress-strain relationship for UHPC, it can be shown that the relationship is almost linear to the peak strength, which is unlike conventional concrete. However, it can be shown that the equivalent rectangular stress block assumed for the design of conventional concrete can be applied to UHPC with negligible error.¹⁴ ACI 318²¹ and the American Association of State Highway and Transportation Officials' *AASHTO LRFD Bridge Design Specifications*²² use the stress block factor β_1 of 0.65 to establish the depth of the equivalent rectangular stress for concrete strength of 8 ksi (55.2 MPa) and higher. It can be shown that this stress block factor β_1 value produces a center of the compression force at 0.33 of the depth to the neutral axis c , which is the same as the center of the compression force produced with the triangular stress distribution. In addition, the total force must, by equilibrium, be the same with the two types of stress distribution. Therefore, as long as the ultimate strain of 0.003 is assumed to be the same for UHPC as for conventional concrete, assuming the equivalent rectangular stress block should produce a nearly identical concrete compression force calculation. Since 1950, it has been traditional to use 0.003 as the ultimate strain, and this value has not changed as concrete strength has increased from 3 to 20 ksi (20.7 to 137.9 MPa). This assumption is used because of its simplicity and because it has virtually no impact on ultimate flexural capacity. When ductility is calculated, a more accurate ultimate strain value may be justifiable. Furthermore, it has been shown in the PCI UHPC project¹⁴ that the tension force is predominated by the contribution of the strands and that fiber contribution to ultimate flexure can conservatively be ignored as long as the prestress level meets the minimum reinforcement requirements in the AASHTO LRFD specifications.²²

Fiber contribution to shear and torsional strength

The most significant contribution to shear strength is the component attributable to the fibers. The recommendations from the PCI UHPC report¹⁴ are used. These recommendations are to apply the current general modified compression field theory (MCFT) from the AASHTO LRFD specifications²² modified to include the fiber contribution. The proposed design equations for the shear strength capacity of UHPC members are included as follows. Using this method, for a member without stirrups, the shear resistance at any given cross section is that of the paste-fiber matrix. Shear resistance may also be contributed by sloped or draped prestressing, if any. While stirrups are discouraged because of the potential for disrupting the flow of fibers, it is possible in some applications to have them at the ends of members subjected to very high shear stresses in a limited part of the total length.

$$V_n = V_{cf} + V_s + V_p \quad (1)$$

where

V_n = nominal shear resistance of the section considered

V_{cf} = nominal shear resistance provided by paste-fiber matrix

V_s = shear resistance provided by shear reinforcement

V_p = component in the direction of the applied shear of the effective prestressing force

$$V_{cf} = \left(\frac{4f_{rr}}{3} \right) b_v d_v \cot \theta \quad (2)$$

where

f_{rr} = postcracking residual tensile strength of the fiber-reinforced cross section

b_v = web width

d_v = effective shear depth

θ = the compression strut angle as calculated in AASHTO

The formulas for shear capacity V_s , compression strut angle θ , longitudinal strain ϵ_s , and minimum longitudinal tension tie ($A_s f_y + A_{ps} f_{ps}$, where A_s is area of nonprestressed tension reinforcement, f_y is specified minimum yield strength of reinforcing steel, A_{ps} is area of prestressing steel, and f_{ps} is average stress in prestressing strand at time for which nominal resistance is required) are the same as given in AASHTO.

The factored demands (factored shear force V_u , factored moment M_u , and factored torsional moment T_u) at the critical section are first calculated using available commercial software. Note that per AASHTO, longitudinal strain ϵ_s is bounded by -0.40×10^{-3} in compression and 6.0×10^{-3} in tension, giving an angle in the range of 27.6 to 50.0 degrees, using AASHTO LRFD specifications Eq. (5.8.3.4.2-3).²²

The most significant contribution to shear strength is the contribution from fibers (nominal shear resistance provided by fibers V_p) combined with aggregates and paste interlock, conventionally called nominal shear resistance of concrete V_c . In the PCI UHPC report,¹⁴ this combined contribution is called V_{cf} . In the recommended calculation method, a post-cracking residual strength of UHPC f_{rr} of 0.75 ksi (5.2 MPa) is recommended as a conservative value based on the extensive full-scale testing described in the PCI UHPC report and recommendations by international researchers and codes. The limit recommended in the PCI UHPC report¹⁴ is also consistent with the philosophies of the Swiss UHPC standard²³ and German UHPC guideline.²⁴

The recommended approach to calculate the concrete contribution V_c is derived from the simplified factor indicating the ability of diagonally cracked concrete to transmit tension and shear (β formula in AASHTO) and the traditional approach of using $2(0.0316)\sqrt{f'_c}$ equal to 0.264 ksi (1.8 MPa) for nonprestressed flexural members and $4(0.0316)\sqrt{f'_c}$ equal to 0.527 ksi (3.6 MPa) for prestressed members, both with a compressive strength of concrete f'_c taken as 17.4 ksi (120 MPa). To conservatively capture the effects of concrete alone without arbitrarily separating it from the contribution of the fibers in the concrete, it is proposed that (0.25 ksi [1.7 MPa]) $\cot \theta$ be used as the concrete contribution, which reduces to 0.25 ksi when θ is 45 degrees and 0.48 ksi (3.3 MPa) when θ is 27.6 degrees. When added to the fiber contribution, the total stress becomes (0.25 ksi + 0.75 ksi) $\cot \theta$, or (1.00 ksi [6.9 MPa]) $\cot \theta$, which happens to equal $(4/3)f_{rr} \cot \theta$.

There is no requirement for minimum transverse reinforcement (stirrups). The minimum amount of steel fibers and the fiber properties would result in fiber-reinforced concrete with adequate strength and strain-hardening properties far exceeding the minimum reinforcement requirements in conventional concrete.

The nominal capacity (resistance) V_n is calculated from Eq. (1), which is the same as AASHTO LRFD specifications Eq. (5.7.3.3-1)²² except that the concrete component is replaced with a paste-fiber composite resistance. Finally, the shear demand is checked against the design capacity, reduced by a resistance factor ϕ of 0.9 in the AASHTO LRFD specifications. This factored capacity ϕV_n should be compared to the factored demand V_u to ensure adequate shear strength in design.

Shear and torsion design

The simplified method used in the AASHTO LRFD specifications²² is adapted in the PCI UHPC report¹⁴ to account for the contribution of the fibers. According to AASHTO LRFD specifications Eq. (5.7.2.1-3), the factored applied torsion should be designed for when it is equal to or greater than $0.25\phi T_{cr}$ and the compatibility torsion can be reduced to ϕT_{cr} to be used in design, where T_{cr} is the torsional cracking moment. Also, the concrete tensile strength represented by the term $0.216\sqrt{f'_c}$ is replaced by the postcracking residual strength of UHPC f_{rr} , which is 0.75 ksi (5.2 MPa) for concrete complying with PCI UHPC minimum properties. Equations (3) and (4) are the modified AASHTO LRFD equations for UHPC.

$$T_u > 0.25\phi T_{cr} \quad (3)$$

For hollow shapes

$$T_{cr} = Kf_{rr} 2A_o b_e \quad (4)$$

where

A_o = area enclosed by the shear flow path, including any area of holes therein

b_e = effective width of the shear flow path taken as the minimum thickness of the exterior webs or flanges composing the closed box section, in which fiber

orientation factor $K = \sqrt{1 + \frac{f_{pc}}{f_{rr}}} \leq 2.0$, where f_{pc} is unfactored compressive stress in concrete after prestress losses have occurred either at the centroid of the cross section resisting transient loads or at the junction of the web and flange where the centroid lies in the flange

After checking the cracking torsion limit, the torsional moment is converted to an equivalent shear force using Eq. (5), which is taken from the AASHTO LRFD specifications. The sum of that shear from torsion and the direct shear produces V_{eff} , which is then used as typical for a member subjected to shear alone.

For hollow shapes

$$V_{eff} = V_u + \frac{T_u d_s}{2A_o} \quad (5)$$

where

V_{eff} = shear force equivalent to combined shear and torsion

d_s = distance from extreme compression fiber to the centroid of the nonprestressed tensile reinforcement which is taken as the full depth of the member h when no torsional reinforcement bars are provided

Design for shear and torsion service limit state is also required. The critical point in the member subject to the highest principal tensile stress should be checked against cracking. This point is

often located near the top of one of the webs next to the support subject to the largest shear and torsion. The allowable stress for this case is recommended to be 0.75 ksi (5.2 MPa), which is a conservative limit based on data from the vast amount of literature and full-scale experimental verifications summarized by the PCI UHPC report.¹⁴ The authors will demonstrate later in this paper that the maximum principal tensile stress is significantly below the limit and no cracking is expected under service loads. Despite the high strength and ductility of UHPC, the authors do not recommend at this time that cracking under service load conditions be allowed until more experience with the material in actual structures is gained.

Structural system description

The UHPC curved bridge system is best described through a numerical design example similar to one recently designed by the authors. The theoretical bridge consists of three spans (120, 240, and 120 ft [36.5, 73, and 36.5 m]), with a 500 ft (152 m) radius curve measured at the centerline of the 50 ft (15 m) width of the bridge (Fig. 4). All components are arranged radially to maintain uniformity. The bridge is framed with four box beams made composite with a precast concrete full-depth, full-width deck panel system (Fig. 5 and 6).

The cross-section dimensions were determined through several design iterations (Fig. 6). Only horizontal (nondraped) post-tensioned strand tendons were used in the bottom flange and the corners of the top flange. This, along with use of UHPC, allows for the elimination of stirrups and reduction of the web width to 4 in. (102 mm) from the standard 9 to 10 in. (229 to 254 mm) required for draped post-tensioned and conventional concrete reinforcing stirrups. The deck panel chosen was 9 in. thick and assumed to be pretensioned transversely in the precasting plant and post-tensioned longitudinally after erection.

The design loads included the weight of the girders, a minimum of 1 in. (25.4 mm) thick haunch, deck panels, and a 2 in.

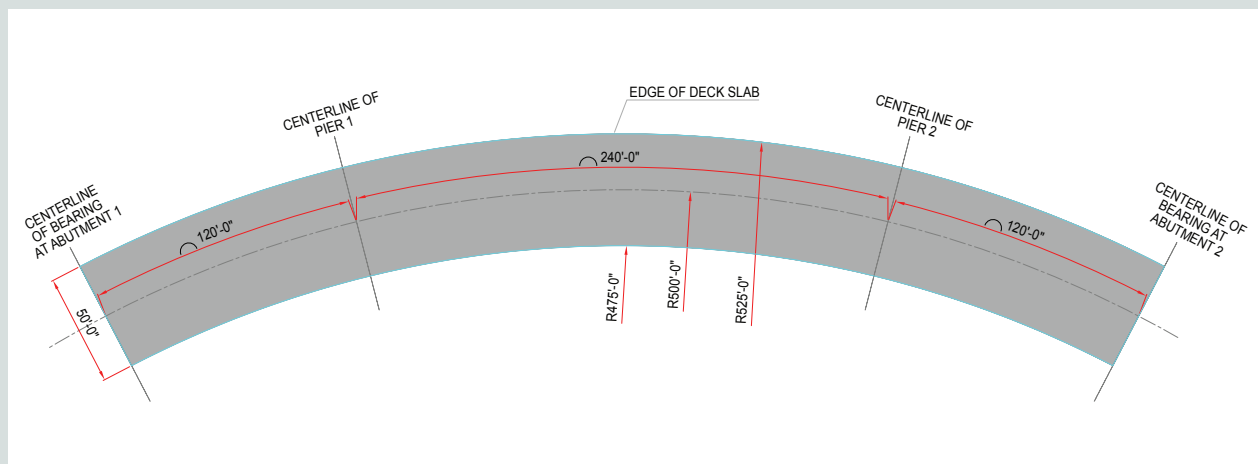


Figure 4. Plan view of the bridge. Note: R = radius. 1" = 1 in. = 25.4 mm; 1' = 1 ft = 0.305 m.

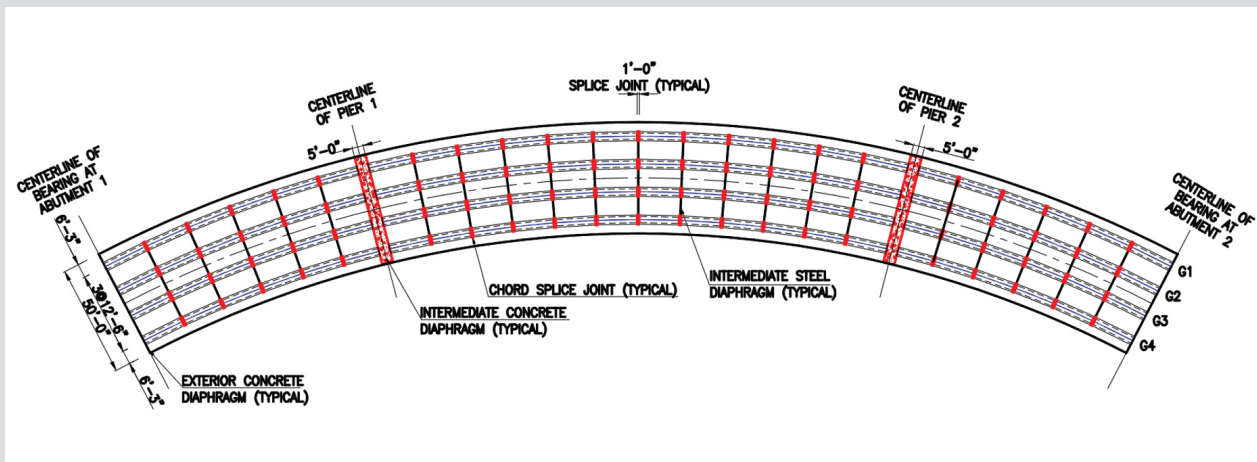


Figure 5. Framing plan and girder numbering. Note: 1" = 1 in. = 25.4 mm; 1' = 1 ft = 0.305 m.

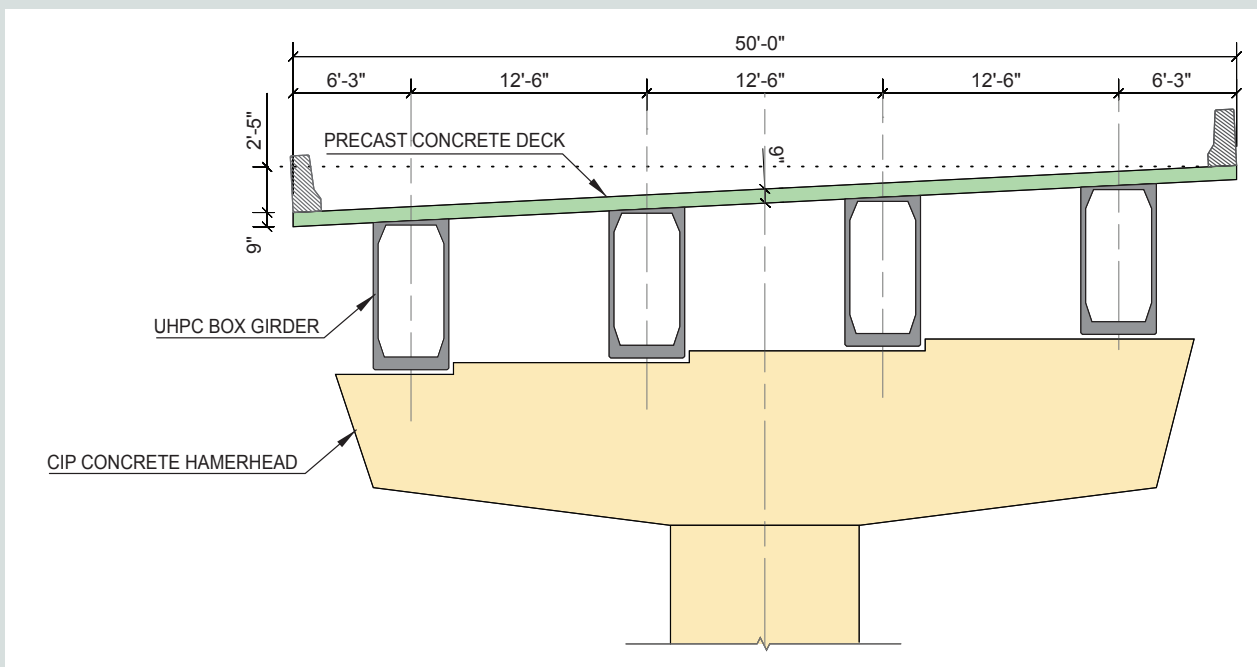


Figure 6. Bridge cross section at the center pier. Note: CIP = cast-in-place; UHPC = ultra-high-performance concrete. 1" = 1 in. = 25.4 mm; 1' = 1 ft = 0.305 m.

(50.8 mm) thick future wearing surface. HL-93 live loads according to the AASHTO LRFD specifications²² were included. Three 12 ft (3.7 m) wide design lanes were assumed.

Design criteria

Design criteria are as generally given in the AASHTO LRFD specifications.²² However, because of the high compressive strength and the presence of steel fibers in the concrete mixture, it is possible to eliminate most of the reinforcement except in disturbed zones. Thus, the primary

provision in the AASHTO LRFD specifications affected by this material is shear design, where an additional strength component is contributed by the fibers. The allowable tensile stress limit in this example was chosen to be 1.0 ksi (6.9 MPa), in accordance with the recommendations of the PCI UHPC report.¹⁴

Flexure Service limit states are as follows:

- compression limit at time of post-tensioning = $0.6f'_c = 6$ ksi and the tension limit = 0.75 ksi (5.2 MPa)

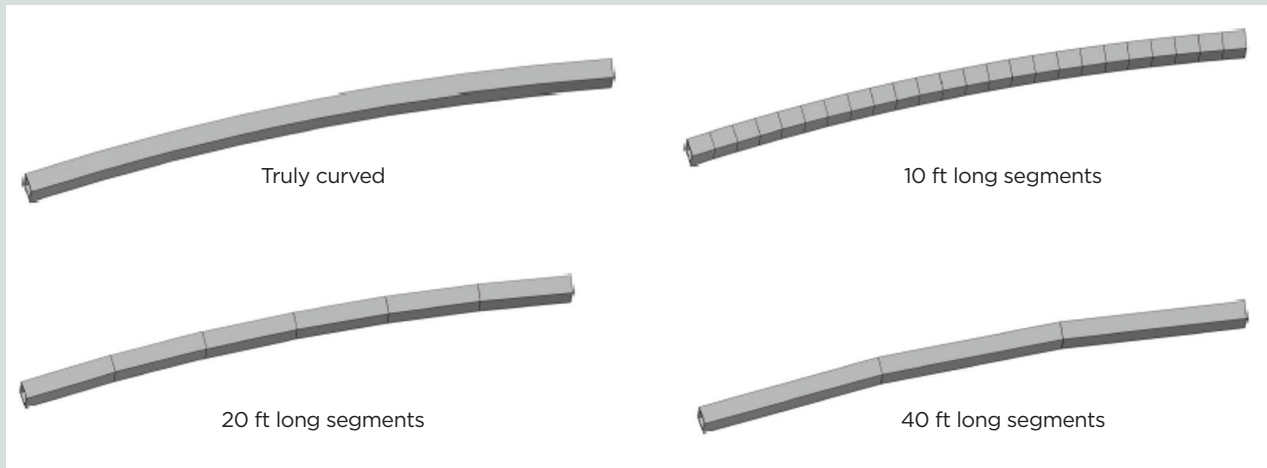


Figure 7. Visual comparison of a 120 ft long span with various segment length options. Note: 1' = 1 ft = 0.305 m.

- compression at final condition due to permanent loads = $0.45f'_c = 7.8$ ksi (53.8 MPa) and due to permanent and transient loads = $0.60f'_c = 10.4$ ksi (71.7 MPa)
- tension at final condition (Service III) = 1.0 ksi (6.9 MPa)

Note that tensile stress at joints should be limited to zero. For the strength limit state, use the strain-compatibility theory with equivalent rectangular stress block and 0.003 extreme face strain and ignore fiber contribution to flexural strength.

Shear For service, limit principal tensile stress to 0.75 ksi (5.2 MPa).

For strength, use MCFT provisions from the AASHTO LRFD specifications.²² The concrete-fiber matrix contribution to shear strength V_{cf} is $1.00 \text{ ksi} \times \text{web width } b_v \times \text{effective shear depth } d_v \times \cot \theta$.

Truly curved versus chorded girders

The number of straight chord segments in each span depends on the span length and degree of curvature. The length of each segment should be 20 ft (6 m) for sharp curvatures and 40 ft (12 m) for mild curvatures, as recommended by the *PCI Bridge Design Manual* (MNL-133-14)⁹ and PCI's *Curved Precast Concrete Bridges State-of-the-Art Report* (CB-01-12).⁸ Using segments shorter than 20 ft is unnecessarily burdensome, though it has been done with special, relatively expensive forms on several Florida bridges. The *PCI Bridge Design Manual* recommends a maximum arc-to-chord offset of 1.5 ft (0.5 m) to have a visually accepted bridge.

For the design example, using 40 ft (12 m) segments on a 500 ft (152 m) radius results in a maximum offset at mid-length of the segment of $L_a^2/8R = 40^2/(8 \times 500) = 0.4$ ft or 4.8 in. (122 mm), where L_a is the arch segment length and

R is the radius of curvature. If the segment length is further reduced to 20 ft (6 m), the resulting offset is 1.2 in. (30.5 mm), which makes it virtually impossible to distinguish the appearance of the chorded structure from a truly curved bridge. As a result, the chorded layout looks like a truly curved girder. Figure 7 shows an illustration of various segmentation options compared with a truly curved girder. An appropriate segmentation option can match a truly curved girder well.

With adequate crane capacity, it is possible to assemble girder segments for the center 240 ft (73 m) span on the ground at the bridge site and lift it in one piece to the pier supports. In this case, the full-span curved segment must have additional supports besides the two end simple-span bearings. The supports may be torsional restraint at the supports or an intermediate shoring tower. The locations of temporary shoring should be decided based on available space away from traffic lanes. It does not need to be at midspan.

For the design example, it is assumed that the end span of the bridge, with six 20 ft (6 m) segments, is assembled and post-tensioned in the precasting plant. It is assumed the center span is assembled in two equal parts in the plant and spliced on the ground at the site. The proposed construction stages are as follows.

Construction sequence

Stage 1: Girder fabrication and transportation Straight segments will be fabricated using straight pretensioning strands to resist their weight. Six segments in each assembly are precisely aligned on a flat concrete bed using the prescribed curvatures for the bridge. Bottom and top post-tensioning tendons, as needed by design, are threaded through the straight ducts embedded in the segments. The ducts are spliced at the open joints (kinks) before closure pours are made.

For the end spans, all top and bottom post-tensioning tendons will be placed and stressed in the precaster's yard. The ducts are grouted before the girders are transported. For the center span, only the post-tensioning tendons required for handling and shipping are inserted and stressed. Once the two halves are set at the site, they are spliced with the center joint and additional post-tensioning for full load. **Figures 8** and **9** illustrate the steps of shipping and field splicing.

To prepare for lifting and handling a 120 ft (36.5 m) long assembly, the lifting points should be carefully identified

such that a straight line linking the lifting points passes through the center of gravity of the girder assembly to minimize possible girder twisting and avoid any stability issue. Similarly, analysis should be performed to determine adequate supports to eliminate any possibility of twisting during transportation. **Figure 10** shows the example details of the side bracing required for torsional resistance once the crane is released.

Stage 2: Girder erection **Figure 11** illustrates erection and torsional restraint of the center-span segment. Side bracing clamps must be secured before the crane is released.



Figure 8. Transporting the six-girder assembly.

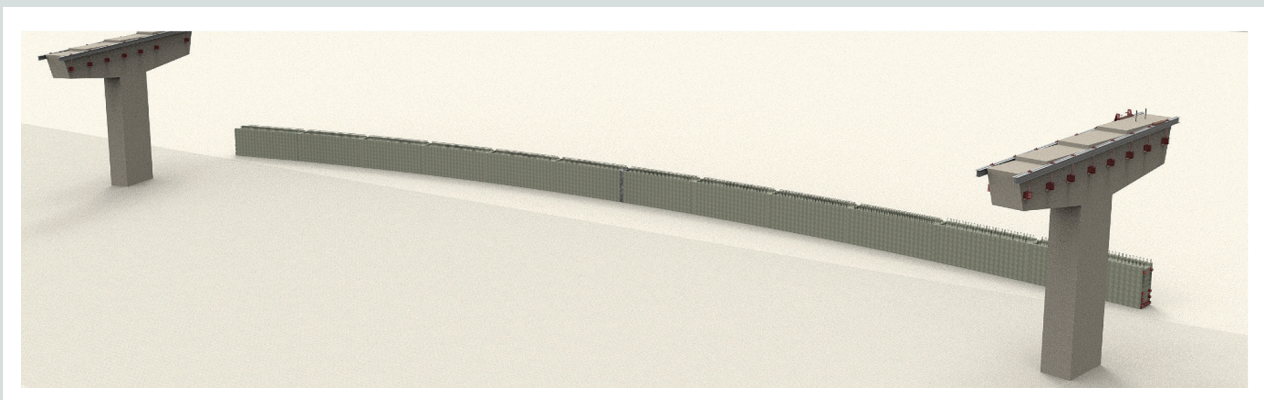


Figure 9. Splicing the two assemblies on ground to form the girder at the center span.

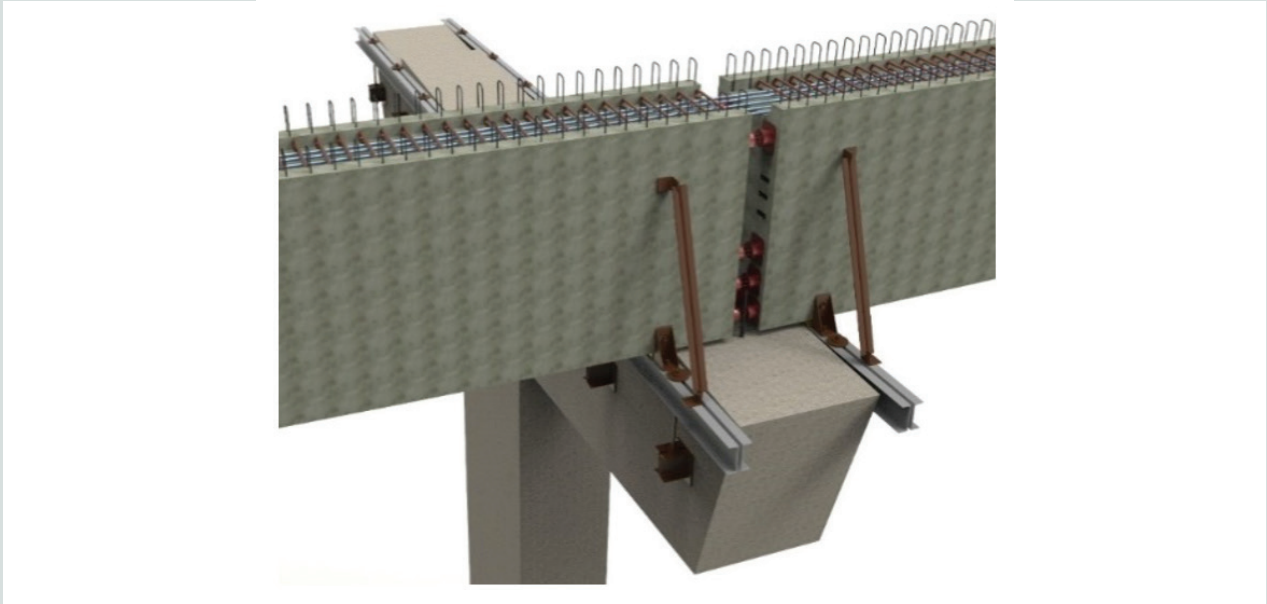


Figure 10. Temporary side bracings at the girder ends.

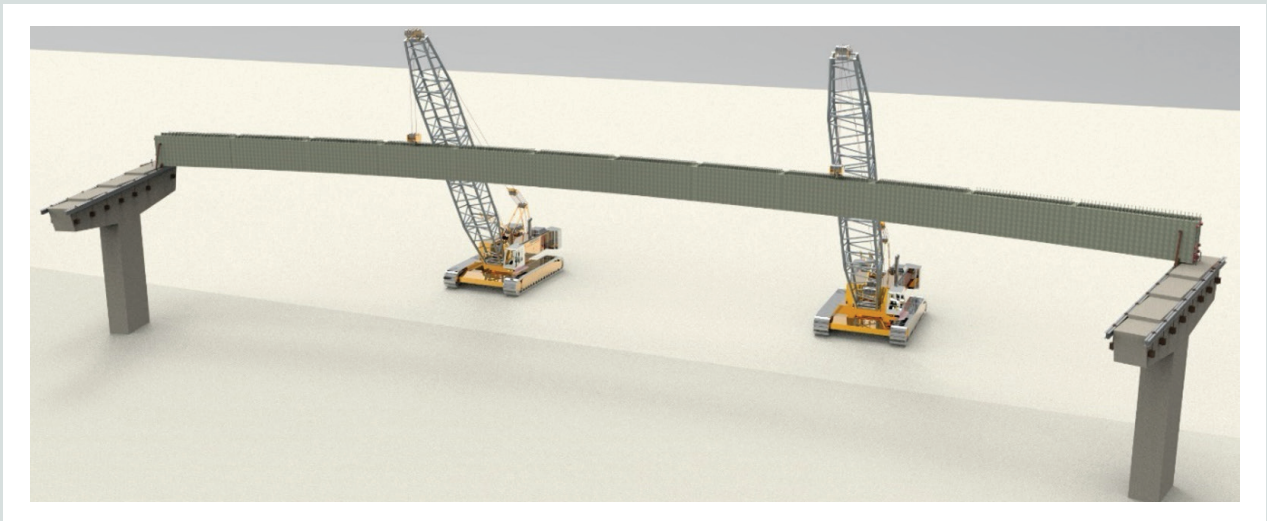


Figure 11. Erecting all segments at the center span.

Stage 3: Erection of steel diaphragms Immediately after erecting the second line of girders, prefabricated steel diaphragms will be used to connect both girder lines at the kink locations. **Figure 12** shows the fully erected girders and diaphragms. Bent plate, X bracing, or K bracing could be used as desired by the designer. The authors prefer the simplicity of the bent plate. Please note the importance of intermediate diaphragms in curved bridge alignment because they are primary, not secondary, members, as assumed for straight alignments.

Stage 4: Placement of concrete in the abutment and pier diaphragms After erecting all girders and intermediate

steel diaphragms, concrete will be placed in the abutment back wall and the pier diaphragms.

Stage 5: Placement of continuity reinforcement and topping over the negative moment zones of the piers High-strength continuity Chrom X 9100 bars (Grade 100 [690 MPa]) will be placed over the piers and covered with 4 in. (102 mm) thick by 4 ft (1.2 m) wide by $L/4$ cast-in-place concrete topping, where L is the span being covered. As will be discussed in this paper, this threaded-rod continuity system has been used successfully on straight bridges in Nebraska, and it is described in detail in Sun et al.²⁵

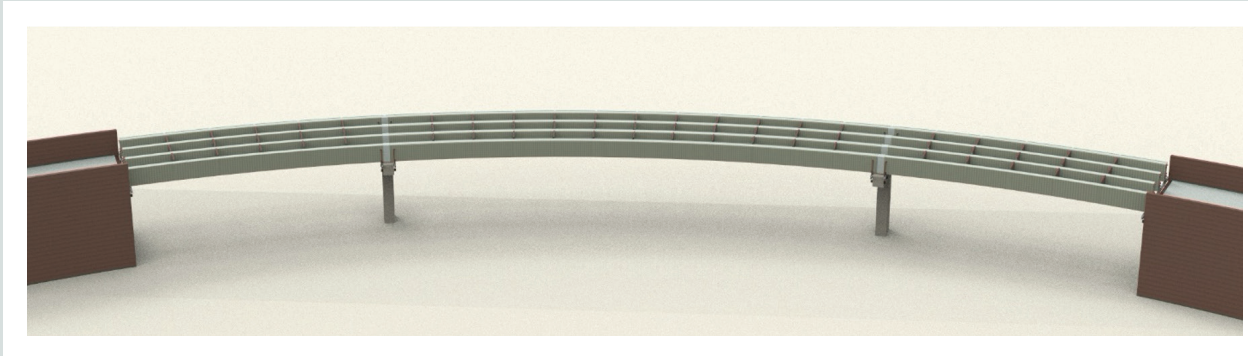


Figure 12. Placing steel diaphragms at the kinked joints, casting concrete diaphragms, and placing high-strength continuity bars over the piers.

Stage 6: Erection of precast concrete deck panels and application of deck post-tensioning After the cast-in-place concrete reaches adequate strength, deck panels will be erected (**Fig. 13**). It is preferable to install the precast concrete deck panels with a pie-shaped layout to allow for consistent cast-in-place joints.

Erection of the deck panels before they are made composite with the girders is a critical stage of loading and must be analyzed carefully. Torsional stresses in the girders due to deck weight and all preceding loads should not exceed the diagonal cracking stress limits using a factor of safety of 1.5. Once the deck panels are made composite with the girders, the composite girders will resist the superimposed dead loads due to railing, overlay weights, and live loads.

The precast concrete panels are then connected to each other by longitudinal post-tensioning and then connected to the girders through pockets in the panels and projecting reinforcing bars from the girders. These details are typical of the construction with full-depth precast concrete panels.^{26,27}

For brevity, design and detailing of the panels and the connection to the girders are not addressed in this paper. It is noteworthy that the precast concrete deck panels themselves can be made of UHPC. If this option were exercised, a very attractive total UHPC superstructure system would be achieved. The weight of the panels would be considerably lighter than conventional concrete because the panels would be ribbed (waffle) slabs consistent with the UHPC deck demonstrated in Iowa.^{28,29}

Methods of analysis of curved stringer bridges

Article 4.1 of the AASHTO LRFD specifications²² requires that analysis be performed using a rational method that accounts for the interaction of the entire superstructure. Small-deflection elastic theory may be used, as for straight stringer bridges. Alawneh¹⁹ demonstrates in detail various methods that can be used in the analysis. They include the approximate V load method by Zureik and Naqib,³⁰ the more detailed two-dimensional (2-D) gridline analysis, and the



Figure 13. Three-dimensional model of the three-span (120, 240, and 120 ft), 50 ft wide bridge with a horizontal curvature radius of 500 ft. The total superstructure, including the 10 ft wide deck, is made of precast concrete components. Note: 1 ft = 0.305 m.

most accurate three-dimensional finite element method. The 2-D model gives reasonably accurate representation of bending moment, shear, and torsion, but it may not be sufficient to provide an accurate evaluation of all reactions and deformations because it ignores the vertical direction in the analysis.

The results given in this paper are based on modeling performed with finite element analysis software. The software allows for modeling the structure as a series of beams, plate elements, or solid elements. It includes the prestress as special

line elements that can be input to follow the alignment of each individual prestressing tendon used.

The exterior girder farthest away from the center of the horizontal curve (referred to here as “exterior girder” for brevity) has the highest bending moments and thus controls the post-tensioning and other details. Analysis of the results of service load bending moment diagrams indicates that the difference in values between the exterior and interior girders is too small to warrant different post-tensioning details.

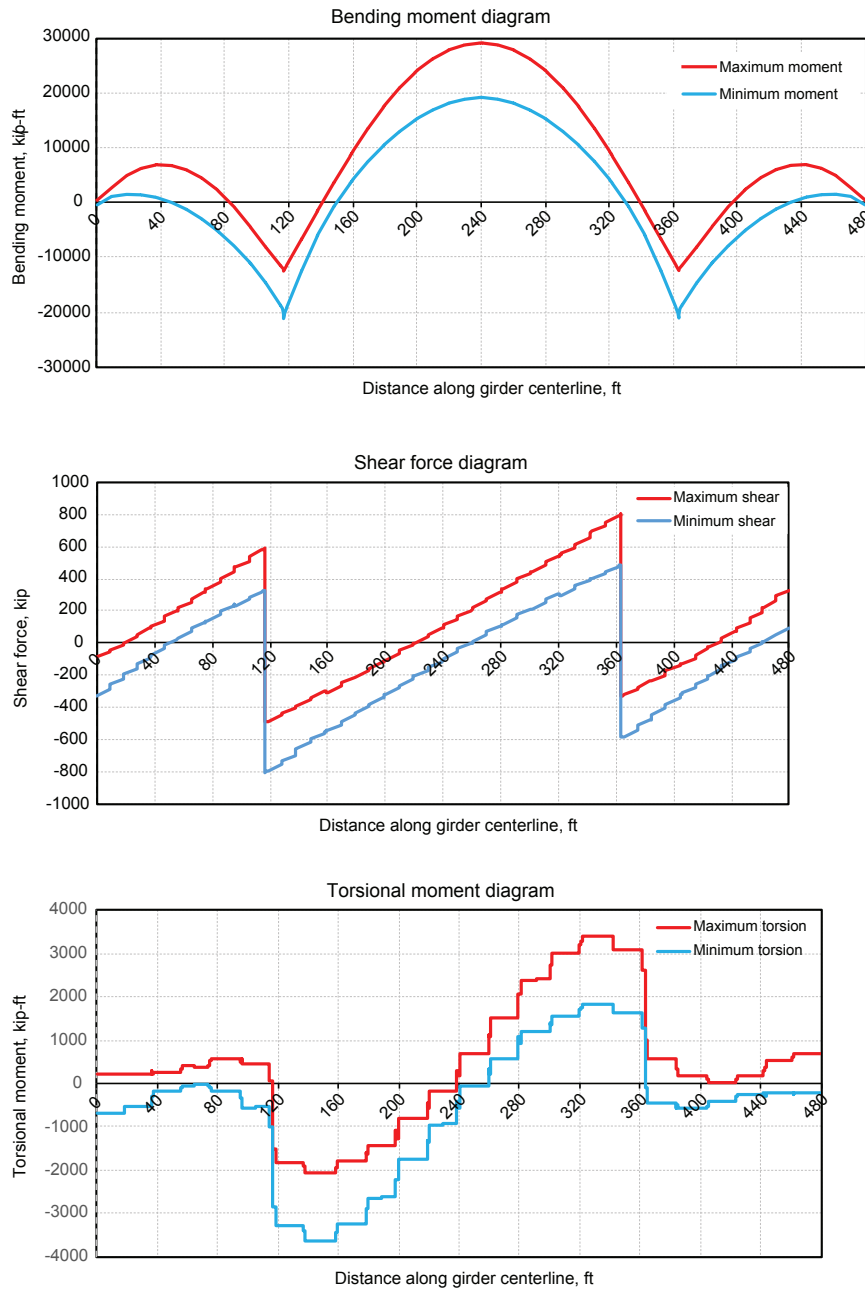


Figure 14. Factored load combination (Strength I) diagrams at the exterior girder. Note: 1 ft = 0.305 m; 1 kip = 4.448 kN; 1 kip-ft = 1.356 kN-m.

Figure 14 shows moment, shear, and torsion due to factored total loads (Strength I) at the exterior girder. The figure illustrates that the maximum moment can vary by as much as 25% between the most exterior and interior girder lines. A complete design must account for all effects in all spans and girder lines while attempting to standardize details. The bending moment, shear, and torsional moment at the critical sections of the center span of the exterior girder are summarized in **Table 1**. Analysis in the following sections will be limited to these values to illustrate the process and to verify adequacy of the selected system.

Flexural design

Flexural design for curved bridges is similar to that for straight bridges once the analysis for load effects is performed with appropriate analysis. All girders are designed with sufficient flexural strength for all loading combinations, as specified in the AASHTO LRFD specifications.²² Construction loads and support conditions are especially important for this type of bridge and frequently control design. Iterations are not shown here. The final cycle satisfies all requirements in the AASHTO LRFD specifications with the selected post-tensioning and the assumed construction stages previously described. **Figure 15** shows the layout of the provided post-tensioning tendons. No cracks are expected under Service I and Service III limit state conditions, including the all-important torsional effects on the precast concrete girder before it is made composite with the deck. **Table 2** shows the stress results, along with flexural demand and capacity, for each construction stage and at two critical sections. Note that the results for the effect of deck erection reflect the fact that the girders are made continuous before the deck panels are erected. Continuity of the girders is achieved by anchoring high-strength bars to the girders in the negative moment zone.

Note that the deck post-tensioning is applied before the deck is connected to the girders. The amount of deck post-tension-

ing is calculated to provide enough precompression force to counteract the 0.63 ksi (4.3 MPa) tensile stresses near the negative zone as well as the required minimum precompression force per the AASHTO LRFD specifications. (Design of the precast concrete deck is not included in this paper for brevity. Readers may refer to the PCI *State-of-the-Art Report on Full-Depth Precast Concrete Bridge Deck Panels*²⁶ and Morcoux and Tadros²⁷ for detailed information on the design of full-depth precast concrete deck slabs.) The top stress in the girder at the negative zone does not control the design because that section is designed as a conventionally reinforced concrete section that uses high-strength reinforcement. Post-tensioning requirements are provided in Fig. 15 and **Fig. 16**.

Strength I shear design procedure

As shown in Table 1, the critical forces at Strength I load combination were calculated as a factored shear force V_u of 804 kip (3576 kN), factored torsional moment T_u of 3713 kip-ft (5034 kN-m), and factored moment M_u of 18,881 kip-ft (25,598 kN-m). The total web width resisting shear force b_v is 8.0 in. (203 mm), the effective depth of the section d_v was calculated to be 101.2 in. (2570 mm), and T_{cr} was calculated using Eq. (4) to be 2736.4 kip-ft (3710 kN-m). **Figure 17** shows a typical cross section with shear and torsional properties. For simplicity, only the box section was considered in torsional analysis. The deck effect can be considered, but its contribution to torsional capacity for the closed box section is insignificant. This is a vastly different behavior from interaction of the deck with U beams, which largely depend on the deck for torsional resistance.

According to Eq. (3), the torsional moment shall be considered in the design when factored torsional moment T_u is greater than $0.25\phi T_{cr}$:

$$0.25 \times 2736.4 \times 0.9 = 616 \text{ kip-ft (835 kN-m)} < T_u = 3713 \text{ kip-ft (5034 kN-m)}$$

torsion must be considered.

Table 1. Internal forces in the center span of the outermost exterior girder

Load case	Load	Midspan			Pier centerline		
		Moment, kip-ft	Shear, kip	Torsion, kip-ft	Moment, kip-ft	Shear, kip	Torsion, kip-ft
1	Girder weight and cross bracing	10,851	0	102	0	-156	-1644
2	Deck weight	5314	0	90	-5775	-173	-254
3	Wearing surface	1015	0	20	-1395	-37	-60
4	Barrier	490	0	10	-675	-18	-30
5	HL-93, maximum	4838	58	224	400	10	272
	HL-93, minimum	-496	-58	-224	-4968	-160	-527
Service III		20,283	58	446	-11,834	-512	-2409
Strength I		29,236	102	674	-18,881	-804	-3713

Note: 1 kip = 4.448 kN; 1 kip-ft = 1.356 kN-m.

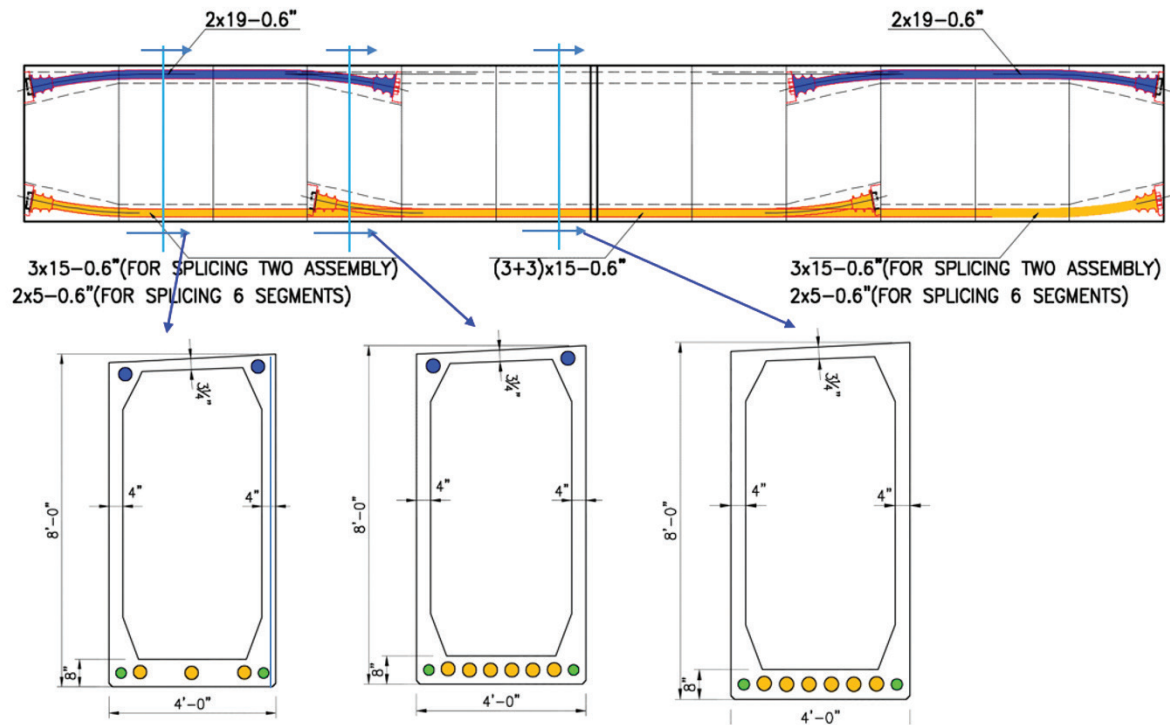


Figure 15. Post-tensioned details for the 240 ft span (temporary post-tensioning bar might be required for handling and erection). Note: 1" = 1 in. = 25.4 mm; 1' = 1 ft = 0.305 m.

Table 2. Flexural design checks at maximum positive and negative moment sections

Load case	At midspan			At pier		
	Girder bottom stresses, ksi [†]	Girder top stresses, ksi	Deck top stresses, ksi	Girder bottom stresses, ksi	Girder top stresses, ksi	Deck top stresses, ksi
Girder weight + post-tensioning	-3.21	-5.96	n/a	-5.55 [‡]	0 [‡]	n/a
Deck slab	+1.39	-1.72	n/a	-1.88	+2.21	-0.25
Wearing surface and barrier	+0.37	-0.18	-0.16	-0.47	+0.22	+0.19
Live load	+1.03	-0.51	-0.47	-1.06	+0.50	+0.44
Service III	-0.42	-8.37	-0.63	-8.96	+2.93	+0.29
Allowable stresses	0.0	-10.8	-10.8	-10.8	n/a	+0.30
Strength I M_u , kip-ft	29,236			-18,881		
Flexural capacity ϕM_n , kip-ft (using bonded post-tensioning tendons)	48,794			-28,734		
Flexural capacity ϕM_n , kip-ft (using external post-tensioning tendons)	32,679			-28,734		

* Sign convention: positive = tension stresses; negative = compression stresses.

[†] Stresses at the bottom of the girder.

[‡] Stresses in the diaphragm; however, the stress at the end of precast concrete section is -2.67 ksi.

^{||} Longitudinal post-tensioning in the deck slab with minimum precompression 0.25 ksi.

Note: M_n = nominal flexural resistance; M_u = factored moment at the section; n/a = not applicable; ϕ = resistance factor. 1 kip-ft = 1.356 kN-m; 1 ksi = 6.895 MPa.

The equivalent vertical shear force $V_{u,eq}$ to account for the effect of torsional moment is calculated at the critical section near the intermediate pier from Eq. (5).

$$V_{u,eq} = V_u + \frac{T_u d_s}{2A_o} = 720 + \frac{3320(12)(103)}{2(4142)} = 1215 \text{ kip (5407 kN)}$$

Note that the value of A_o used in this equation is calculated for a composite section, which is greater than the value shown in Fig. 17.

The longitudinal strain at the center of the tension reinforcement was found to be negative. Conservatively, its value is taken as zero. Accordingly, θ was calculated to be 29 degrees. The concrete shear strength including the contribution of the steel fiber is calculated from Eq. (2) as follows.

$$V_{cf} = \left(\frac{4f_{rr}}{3} \right) b_v d_v \cot \theta = 1.0(8)(101.2)(\cot 29) = 1457.3 \text{ kip (6482 kN)}$$

Thus, the nominal shear strength is calculated as follows:

$$V_n = \phi V_{cf} = 0.9(1457.3) = 1311.6 \text{ kip} > V_{u,eq} = 1215 \text{ kip}$$

Check the adequacy of tension tie by satisfying Eq. (7.9.4-1) from the PCI UHPC report.¹⁴

$$A_s + A_{ps} f_{ps} \geq \left(\frac{V_u}{\phi_v} \right) \cot \theta \quad (7.9.4-1)$$

where

ϕ_v = angle of inclination of diagonal compressive stresses

$$6 \times 15 \times 0.217 \times 180 = 3515.4 \text{ kip (15,363 kN)} > (1215/0.9) (\cot 29) = 2436 \text{ kip (10,838 kN)} \quad \mathbf{OK}$$

Service I shear design procedure

The shear stress due to vertical shear can be calculated by dividing the total shear force by the web area, which will provide the average shear stresses along the depth of the section as per AASHTO LRFD specifications Eq. (5.8.2.9-1):

$$\tau = \frac{V}{b_w h} = \frac{458}{8(105)} = 0.54 \text{ ksi (3.72 MPa)}$$

where

τ_v = shear stress due to vertical shear force

V = vertical shear force

b_w = web width

Torsion shear stress is calculated from first principle of mechanics assuming no cracking:

$$\tau = \frac{T}{2A_o t} = \frac{2144(12)}{2(4142)(4)} = 0.77 \text{ ksi (5.35 MPa)}$$

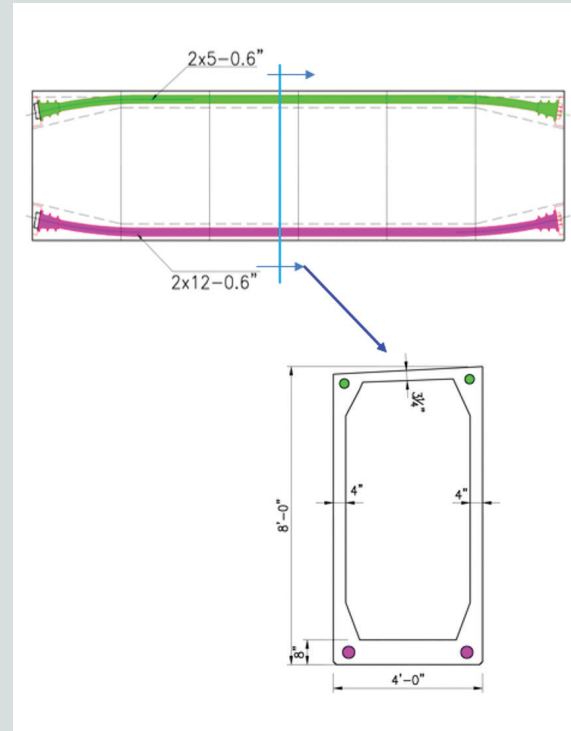


Figure 16. Post-tensioned details for 120 ft span. Note: 1" = 1 in. = 25.4 mm; 1' = 1 ft = 0.305 m.

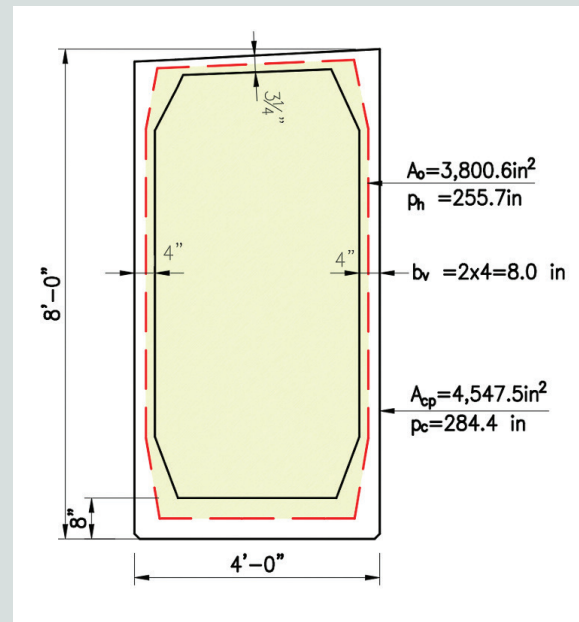


Figure 17. Torsional properties for typical noncomposite section. Note: A_{cp} = area enclosed by outside perimeter of concrete cross-section; A_o = area enclosed by shear flow path; b_v = width of web; p_c = length of the outside perimeter of the concrete section; p_h = perimeter of the centerline of the closed transverse torsion reinforcement. 1" = 1 in. = 25.4 mm; 1' = 1 ft = 0.305 m.

where

τ = shear stress in web vertical shear

t = wall thickness

T = applied torsional moment

Total shear stresses = $0.54 + 0.77 = 1.31$ ksi (9.0 MPa)

Flexural stresses due to negative moment at critical section was calculated -8.96 ksi (61.8 MPa) (compression) and 0.29 ksi (1.8 MPa) (tension), at the bottom and top of the box section, respectively.

Principal tensile stress =

$$\frac{\sigma_x}{2} \pm \sqrt{\left(\frac{\sigma_x}{2}\right)^2 + (\tau_{xy})^2} = \frac{0.29}{2} \pm \sqrt{\left(\frac{0.29}{2}\right)^2 + (1.31)^2}$$

$$= 1.46 \text{ ksi (9.96 MPa)} > 0.75 \text{ ksi (5.2 MPa)}$$

where

σ_x = axial stress along longitudinal axis for the member

τ_{xy} = shear stress

Because the principal tensile stress is greater than 0.75 ksi (5.2 MPa) the web width near the support in the main span must be widened to provide adequate safety against diagonal cracking at service load.

Table 3 shows a comparison of the primary material quantities in precast, prestressed concrete girders between this design example and similar design previously performed by the authors. The Wekiva Bridge had comparable spans and bridge width. It involved use of a conventional concrete spliced girder. When UHPC is used, there is considerable savings in material quantities, including a near elimination of reinforcing bars and a significant reduction in post-tensioning. Also, production labor is greatly reduced and the need for heavy equipment is minimized. Life-cycle analysis has not been performed, but the authors are confident that using UHPC would demonstrate much higher value.

Conclusion

This paper is intended to demonstrate the viability and effectiveness of employing UHPC in curved bridges and to show that precast UHPC production can be standardized. Forming and shoring costs can be significantly reduced by using long UHPC segments. A numerical example of a three-span bridge with a maximum span of 240 ft (73 m) and a sharp curvature of 500 ft (152 m) was presented to address the primary design criteria and production and constriction considerations. The presentation in the paper is intended to be a preliminary concept design to demonstrate the great value presented by UHPC. Compared with a design previously performed by the authors on a bridge with similar spans, width, and curvature, one-third of the concrete and post-tensioning strands can be saved and nearly three-quarters of the reinforcing bars can be eliminated as shown in Table 3.

The design recommendations for UHPC in flexure, shear, and torsion are based on recommendations given in the PCI-sponsored study on implementation of UHPC in long-span building and bridge members. The study was based on findings reported in literature published worldwide and on international recommendations from France,³¹ Korea,³² Australia,³³ and Japan.³⁴ The PCI UHPC report¹⁴ included extensive full-scale testing by four major structural testing laboratories.

An attractive contribution to the optimization of the proposed system is the full-depth precast concrete longitudinally post-tensioned deck system. It can be designed and detailed to be modular, and thus highly efficient, due to the geometry of the structure.

Acknowledgments

The authors are grateful to George Morcoux for his significant contributions to the subject. He was the primary supervisor of Musa Alawneh in his doctorate program and graciously supervised an extensive full-scale testing program by Alawneh. Gregg Reese reviewed and provided thoughtful comments on early versions of this paper. Special thanks go to Mostafa Abo Elkhier for providing technical review. Finally, the authors are grateful to e.construct for sponsoring Alawneh's PhD studies and, in particular, to e.construct's general manager Nader Jaber for his leadership and foresight.

Table 3. Comparison of material quantities between ultra-high-performance concrete and conventional concrete options

Quantity	UHPC curved bridge, A	Conventional precast concrete curved bridge, B	Ratio = A/B
Concrete, yd ³	657	989	0.66
Post-tensioning strand, lb	100,000	160,493	0.62
Reinforcing bars, lb	32,400	145,946	0.22

Note: UHPC = ultra-high-performance concrete. 1 lb = 4.448 N; 1 yd³ = 0.765 m³.

References

1. SSRC (Structural Stability Research Council) Task Group 14. 1991. "A Look to the Future." In *Report of Workshop on Horizontally Curved Girders*. Chicago, IL: SSRC.
2. ABAM Engineers. 1988. "Special Report: Precast Prestressed Concrete Horizontally Curved Bridge Beams." *PCI Journal* 33 (5): 50–95. https://www.pci.org/PCI_Docs/Design_Resources/Guides_and_manuals/references/bridge_design_manual/JL-88-September-October_Precast_Prestressed_Concrete_Horizontally_Curved_Bridge_Beams.pdf.
3. Endicott, W. A. 2005. "A Fast Learning Curve." *Ascent* (Summer): 36–39.
4. Shutt, C. A. 2012. "Curved, Spliced, U-Girders Gain Momentum." *Aspire* 6 (4): 13. <http://www.aspirebridge.com/magazine/2012Fall/CCC.pdf>.
5. Forars, K. P., A. Wolek, J. Alkhub, D. N. Pretorius, and T. E. Davidson. 2014. "Design and Construction of Florida's First Spliced Curved Concrete U-Girder Bridges: The SR 417 and Boggy Creek Road Interchange." In *Proceedings, 60th Anniversary Convention and National Bridge Conference, Washington, DC*. Chicago, IL: PCI. CD-ROM.
6. Sun, C., S. Hennessey, M. Ahlman, and M. Tadros. 2007. "Value Engineering Arbor Road Bridge with Curved Precast Concrete Girders." *PCI Journal* 52 (2): 94–106.
7. McMullen, M. L., J. I. Elkaissi, and M. A. Leonard. 2008. "Long-Span Precast U-Girders in Colorado." *Aspire* 2 (4): 64–67. http://www.aspirebridge.com/magazine/2008Fall/state_CO_fall08.pdf.
8. PCI Committee on Bridges. 2012. *Curved Precast Concrete Bridges State-of-the-Art Report*. CB-01-12. Chicago, IL: PCI.
9. PCI. 2014. *Bridge Design Manual*. MNL-133-14. 3rd ed. Chicago, IL: PCI.
10. Mohseni, M. M., K. Saindon, and C. Krajnik. 2014. "Colorado Flyover Ramp Showcases Precast Pier Caps and Curved Spliced Precast U-Girders." Webinar. Accelerated Bridge Construction Center, Florida International University. Recorded December 18, 2014. <https://abc-utc.fiu.edu/mc-events/colorado-flyover-ramp-showcases-precast-pier-caps-and-curved-spliced-precast-u-girders>.
11. Alawneh, M., M. K. Tadros, G. Morcous. 2016. "Innovative System for Curved Precast Posttensioned Concrete I-Girder and U-Girder Bridges." *ASCE Journal of Bridge Engineering* 21 (11). [https://doi.org/10.1061/\(ASCE\)BE.1943-5592.0000938](https://doi.org/10.1061/(ASCE)BE.1943-5592.0000938).
12. Pfeifer, C., B. Moeser, C. Giebson, and J. Stark. 2009. "Durability of Ultra-High-Performance Concrete." In *10th ACI International Conference on Recent Advances in Concrete Technology and Sustainability Issues*, ACI (American Concrete Institute) Special Publication 261. Farmington Hills, MI: ACI.
13. Russell, H. G., and B. A. Graybeal. 2013. *Ultra-High-Performance Concrete: A State-of-Art Report for the Bridge Community*. FHWA/HRT-13-060. McLean, VA: (FHWA Federal Highway Administration).
14. Tadros, M. K., John Lawler, Mostafa Abo El-Khier, David Gee, Atilla Kurt, Gregory Lucier, and Elizabeth Wagner. 2021. *Implementation of Ultra-High Performance Concrete in Long-Span Precast Pretensioned Elements for Concrete Buildings and Bridges: Phase II Report*. Chicago, IL: PCI. <https://doi.org/10.15554/pci.rr.mat-013>.
15. Voo, Y. L., W. K. Poon, and S. J. Foster. 2010. "Shear Strength of Steel Fiber-Reinforced Ultrahigh-Performance Concrete Beams without Stirrups." *Journal of Structural Engineering* 136 (11): 1393–1400. [https://doi.org/10.1061/\(ASCE\)ST.1943-541X.0000234](https://doi.org/10.1061/(ASCE)ST.1943-541X.0000234).
16. ASTM International. 2019. *Standard Test Method for Flexural Performance of Fiber-Reinforced Concrete (Using Beam With Third-Point Loading)*. ASTM C1609/C1609M-12. West Conshohocken, PA: ASTM International. https://doi.org/10.1520/C1609_C1609M-12.
17. ASTM International. 2020. *Standard Specification for Deformed and Plain Carbon-Steel Bars for Concrete Reinforcement*. ASTM A615/A615M-20. West Conshohocken, PA: ASTM International. https://doi.org/10.1520/A0615_A0615M-20.
18. ASTM International. 2020. *Standard Specification for Deformed and Plain, Low-Carbon, Chromium, Steel Bars for Concrete Reinforcement*. ASTM A1035/1035M-20. West Conshohocken, PA: ASTM International. https://doi.org/10.1520/A1035_A1035M-20.
19. Alawneh, M. 2013. "Curved Precast Prestressed Concrete Girder Bridges," PhD diss., University of Nebraska–Lincoln.
20. Gowripalan, N., and R. I. Gilbert. 2000. *Design Guidelines for RPC Prestressed Concrete Beams*. Sydney, Australia: VSL (Australia) Pty. Ltd.
21. ACI. 2019. *Building Code Requirements for Structural Concrete (AC 318-19) and Commentary (ACI 318R-19)*. Farmington Hills, MI: ACI.
22. AASHTO (American Association of State Highway and Transportation Officials). 2020. *AASHTO LRFD Bridge Design Specifications*. 9th ed. Washington, DC: AASHTO.

23. SIA (Swiss Society of Engineers and Architects). 2016. *Standard: Ultra-High Performance Fiber Reinforced Cement-Based Composites (UHPRFC)*. English translation of the Technical Leaflet SIA 2052 with adaptations. Lausanne, Switzerland: Ecole Polytechnique Fédérale de Lausanne Structural Maintenance and Safety Laboratory.
24. DAfStb (Deutscher Ausschuss für Stahlbeton). 2017. *Ultra-High-Performance Concrete*. Berlin, Germany: DAfStb.
25. Sun, C., N. Wang, M. K. Tadros, A. F. Girgis, and F. Jaber. 2016. "Threaded Rod Continuity for Bridge Deck Weight." *PCI Journal* 61 (3): 47–67. <https://doi.org/10.15554/pcij61.3-03>.
26. PCI Committee on Bridges and PCI Bridge Producers Committee. 2011. *State-of-the-Art Report on Full-Depth Precast Concrete Bridge Deck Panels*. SOA-01-1911E. Chicago, IL: PCI. <https://doi.org/10.15554/SOA-01-1911>.
27. Morcoux, G., and M. K. Tadros. 2013. *Implementation of Precast Concrete Deck System NUDECK (2nd Generation)*. SPR-P1 (13) M323. Omaha, NE: Nebraska Department of Roads. <https://dot.nebraska.gov/media/5700/final-report-m323.pdf>.
28. Honarvar, E., S. Sritharan, J. Matthews Rouse, and S. Aaleti. 2015. "Bridge Decks with Precast UHPC Waffle Panels: A Field Evaluation and Design Optimization." *Journal of Bridge Engineering* 21 (1): 04015030. [https://doi.org/10.1061/\(ASCE\)BE.1943-5592.0000775](https://doi.org/10.1061/(ASCE)BE.1943-5592.0000775).
29. Aaleti, S., S. Sritharan, D. Bierwagen, and T. Wipf. 2011. "Experimental Evaluation of Structural Behavior of Precast UHPC Waffle Bridge Deck Panels and Connections." In *Proceedings, Transportation Research Board Annual Meeting, Washington, DC*. Washington, DC: Transportation Research Board.
30. Zureick, A., and R. Naqib. 1999. "Horizontally Curved Steel I-Girder State-of-the-Art Analysis Methods." *Journal of Bridge Engineering* 4 (1): 38–47.
31. AFGC (Association Française de Génie Civil). 2002. *Ultra-High Performance Fibre-Reinforced Concretes, Interim Recommendations*. Paris, France: AFGC.
32. KICT (Korea Institute of Civil Engineering and Building Technology). 2012. *Guidelines for K-UHPC Structural Design*. Gyeonggi-do, South Korea: KICT.
33. Gowripalan, N., and I. R. Gilbert. 2000. *Design Guidelines for Ductal Prestressed Concrete Beams*. Sydney, Australia: University of New South Wales.
34. JSCE (Japan Society of Civil Engineers). 2008. *Recommendations for Design and Construction of High Performance Fiber Reinforced Cement Composites with Multiple Fine Cracks (HPFRCC)*. Tokyo, Japan: JSCE.

Notation

a	= depth of equivalent rectangular stress block
A_{cp}	= area enclosed by outside perimeter of concrete cross section, including area of holes, if any
A_o	= area enclosed by shear flow path, including area of holes, if any
A_{ps}	= area of prestressing steel
A_s	= area of nonprestressed tension reinforcement
b_e	= effective width of the shear flow path
b_v	= effective web width taken as the minimum web width
b_w	= web width
c	= distance from the extreme compression fiber to the neutral axis
d_s	= distance from extreme compression fiber to the centroid of the nonprestressed tensile reinforcement
d_v	= effective shear depth taken as the distance measured perpendicular to the neutral axis between the resultants of the tensile and compressive forces
E_s	= modulus of elasticity of steel reinforcement
f	= beam stresses at the extreme fibers
f'_c	= compressive strength of concrete for use in design
$\sqrt{f'_c}$	= design concrete compressive strength at time of prestressing for pretensioned members and at time of initial loading for nonprestressed members
f_f	= tensile stress corresponding to certain load during the flexural strength test in accordance with ASTM C1609
f_{fc}	= tensile strength at first cracking
f_{fu}	= peak tensile strength
f_{pc}	= compressive stress in concrete after all prestress losses have occurred either at the centroid of the cross section resisting live load or at the junction of the web and flange when the centroid lies in the flange

f_{ps}	= average stress in prestressing strand at time for which nominal resistance is required	V_s	= shear resistance provided by transverse reinforcement
f_{rr}	= postcracking residual tensile strength of the fiber-reinforced cross section	V_u	= factored shear force
f_y	= specified minimum yield strength of reinforcing steel	$V_{u,eq}$	= equivalent vertical shear force accounting for the effect of torsional moment
h	= overall depth of the beam	β	= factor indicating the ability of diagonally cracked concrete to transmit tension and shear (a value indicating concrete contribution to shear resistance)
K	= fiber orientation factor	β_1	= stress block factor
L	= total specimen length for testing in accordance with ASTM C1609	ϵ_s	= net longitudinal tensile strain at the centroid of the tension reinforcement
L_a	= arc length	σ_x	= axial stresses along x direction
L_c	= distance between supports of specimen tested in accordance with ASTM C1609	τ	= shear stress in web vertical shear
M	= unfactored bending moment	τ_v	= shear stress due to shear force in y direction
M_n	= nominal flexural resistance	τ_{xy}	= shear stresses
M_u	= factored moment at the section	ϕ	= resistance factor
p_c	= permanent net compressive force	ϕ_v	= angle of inclination of diagonal compressive stresses
p_h	= perimeter of the centerline of the closed transverse torsion reinforcement		
R	= radius of curvature		
S	= section modulus		
t	= wall thickness for box section		
T	= unfactored torsional moment		
T_{cr}	= torsional cracking resistance		
T_u	= factored torsional moment		
V	= unfactored shear force		
V_c	= nominal shear resistance of the concrete		
V_{cf}	= concrete-fiber matrix contribution to shear strength		
V_{eff}	= shear force equivalent to combined shear and torsion		
V_f	= nominal shear resistance provided by fibers		
V_n	= nominal shear resistance		
V_p	= component of prestressing force in the direction of the shear force		

About the authors



Musa Alawneh is a design manager at e.construct FZ-LLC in Dubai, United Arab Emirates.



Maher Tadros, PhD, PE, is a founding principal of e.construct USA LLC. He is a distinguished emeritus professor, a PCI Medal of Honor recipient, and principal author of PCI-UHPC Structures Design Guide.



Chuanbing (Shawn) Sun, PhD, PE, is an assistant professor in the Department of Civil Engineering and Construction Management at California State University, Northridge.

Abstract

Horizontally curved bridges have been mostly built with steel plate I-girders or tub girders. In the past 15 years, curved concrete girders have been successfully used in several states, including Nebraska, Colorado, and Florida. This paper addresses the design of curved concrete girder bridges using ultra-high-performance concrete (UHPC) by combining state-of-the-art spliced girder technology and UHPC technology. It also proposes a number of unique features that result in further simplification of precast concrete production and construction. Critical design criteria are discussed. The system development of curved UHPC girder bridges and necessary construction steps are elaborated through a numerical example of a three-span bridge, which shows greatly reduced concrete quantities when compared with recently constructed curved concrete girders. With UHPC designed as proposed here, horizontally curved bridges are expected to be cost competitive with conventional concrete and more economical than structural steel.

Keywords

Curved bridge, post-tensioned concrete, steel fiber, torsion, UHPC, ultra-high-performance concrete.

Review policy

This paper was reviewed in accordance with the Precast/Prestressed Concrete Institute's peer-review process. The Precast/Prestressed Concrete Institute is not responsible for statements made by authors of papers in *PCI Journal*. No payment is offered.

Publishing details

This paper appears in *PCI Journal* (ISSN 0887-9672) V. 67, No. 2, March–April 2022, and can be found at <https://doi.org/10.15554/pcij67.2-02>. *PCI Journal* is published bimonthly by the Precast/Prestressed Concrete Institute, 8770 W. Bryn Mawr Ave., Suite 1150, Chicago, IL 60631. Copyright © 2022, Precast/Prestressed Concrete Institute.

Reader comments

Please address any reader comments to *PCI Journal* editor-in-chief Tom Klemens at tklemens@pci.org or Precast/Prestressed Concrete Institute, c/o *PCI Journal*, 8770 W. Bryn Mawr Ave., Suite 1150, Chicago, IL 60631. 